Biosensors and Bioelectronics 169 (2020) 112651

Contents lists available at ScienceDirect

Biosensors and Bioelectronics

journal homepage: http://www.elsevier.com/locate/bios

An IoT-enabled paper sensor platform for real-time analysis of isothermal nucleic acid amplification tests

Mingdian Liu [a], Yuxin Zhao [b], Hosein Monshat [c], Zheyuan Tang [a], Zuowei Wu [d], Qijing Zhang [d], Meng Lu [a,c,*]

[a] Department of Electrical and Computer Engineering, Iowa State University, Ames, IA, 50011, USA
[b] Department of Chemical and Biological Engineering, Iowa State University, Ames, IA, 50011, USA
[c] Department of Mechanical Engineering, Iowa State University, Ames, IA, 50011, USA
[d] Department of Veterinary Microbiology and Preventive Medicine, Iowa State University, Ames, IA, 50011, USA

ARTICLE INFO

Keywords:
IoT
Paper-based sensor
Isothermal PCR
Pathogens
Bacteria

ABSTRACT

Paper-based sensors can be exploited to develop low-cost, disposable, and rapid assays for the detection of a large variety of analytes. We report a paper-based sensor system for a point-of-care (POC) nucleic acid amplification test that can quantitatively detect multiple genes from different pathogens. The POC system combines a paper sensor chip and a portable instrument, which is built on an Internet of Things (IoT) platform. The paper-based sensor provides the functions of reagent storage, sample transportation, and nucleic acid amplification. The IoT instrument uses an Arduino microcontroller to control temperature, collect fluorescence images, and store the data in cloud storage *via* a WiFi network. A compact fluorescence reader was designed to measure fluorescence images of the amplicons during a loop-mediated isothermal amplification reaction in real-time. The real-time detection capability enables the quantitative analysis of target genes. The results show that the paper-based sensor cam distinguish multiple genes of the genomic DNA extracted from Escherichia coli and Campylobacter jejuni, with the concentration as low as 2×10^3 copies/μL. The affordable instrument, in conjunction with the disposable paper sensor chip, would have a great potential for POC detections of pathogens.

1. Introduction

There are substantial advantages to implement nucleic acid amplification tests (NAATs) in point-of-care (POC) testing systems for rapid diagnosis of diseases, such as bacterial and viral infections (Kiechle and Holland, 2009; Niemz et al., 2011). A patient-side NAAT technology allows primary care physicians to obtain testing results and provide specific treatment promptly (Cordray and Richards-Kortum, 2012; Lee et al., 2010). For example, lab-on-a-chip systems have been successfully developed by integrating DNA amplification and detection function on the same chip (Burns et al., 1998; Lee et al., 2008). More recently, isothermal polymerase chain reactions (PCRs), such as the loop-mediated isothermal amplification (LAMP) and recombinase polymerase amplification (RPA), have been investigated for the POC diagnostic applications (Craw and Balachandran, 2012; Petralia and Conoci, 2017; St John and Price, 2014). Since the isothermal PCRs can be performed at a lower temperature and without temperature cycling, the isothermal PCR assays are highly desirable in most POC platforms, in particular, paper-based sensors.

The paper-based sensors have been studied as a low-cost alternative to conventional microfluidics for POC applications (Bedin et al., 2017; Chan et al., 2013; Choi et al., 2016; Chu et al., 2020; Hu et al., 2014; Kaur and Toley, 2018; Li et al., 2011; Magro et al., 2017; Shah et al., 2013; Syedmoradi and Gomez, 2017; Wang et al., 2020, 2019; 2017, 2016; Yan et al., 2012; Yetisen et al., 2013). The porous feature of paper substrates offers the capability of capillarity-driven sample flow and long-term storage of reagents in paper. Many molecular diagnostic assays, such as lateral flow assay, enzyme-linked absorbance assay, and PCR assays, have been reported using paper-based sensors for the testing of proteins, nucleic acids, and chemical compounds (Cheng et al., 2010; Cinti et al., 2017a, 2017b; Ge et al., 2014; Hossain et al., 2009; Li et al., 2013; Parolo and Merkoçi, 2013; Yu et al., 2011; Zhang et al., 2015; Zhao et al., 2013; Zhou et al., 2014). The assay output can be read using colorimetric, fluorescent, Raman scattering, and electrochemical signals. The development of paper microfluidics further enriched the paper-based assays. Lafleur et al. showed the paper-based bacteria lysis,

* Corresponding author. Department of Electrical and Computer Engineering, Iowa State University, Ames, IA, 50011, USA.
E-mail address: menglu@iastate.edu (M. Lu).

https://doi.org/10.1016/j.bios.2020.112651
Received 29 July 2020; Received in revised form 2 September 2020; Accepted 23 September 2020
Available online 24 September 2020

DNA extraction, and detection using a paper microfluidic device (Lafleur et al., 2016). Seok et al. demonstrated the paper-based LAMP assay, which operated at 65 °C and measured fluorescence intensities at the end of the LAMP amplification (Seok et al., 2017). Gootenberg et al. developed the specific high-sensitivity enzymatic reporter unlocking (SHERLOCK) technology that combined RPA and CRISPR-Cas13 to detect RNA or DNA from clinically samples *via* fluorescence and colorimetric readouts (Gootenberg et al., 2018).

To achieve a quantitative NAAT assay, the real-time detection of PCR products plays a key role in generating the amplification curves during an amplification process. To date, the real-time NAAT analysis using a paper substrate is still an unfulfilled task. To address the challenge, this work implemented an inexpensive and compact NAAT sensor system that uses an IoT-based fluorescence detector to facilitate the paper-based LAMP assay. To detect multiplex genes simultaneously, the paper-based sensor chip was designed to store LAMP reagents and primers in paper reaction pads and transport samples *via* paper fluidic channels. The portable LAMP detector, consisting of a temperature controller, fluorescent detector, and an IoT microprocessor was implemented for automatic data collection, storage over the cloud, and analysis. The system was successfully applied to detect genes from two Gram-negative bacteria: *Escherichia coli* (*E. coli*) and *Campylobacter jejuni* (*C. jejuni*).

2. Material and methods

2.1. Materials and reagents

The cellulose filter paper (CFP1), polyethersulfone membrane (PES509025), and glass microfiber paper (28297-984) were purchased from Whatman plc, Sterlitech Corp., and VWR International, independently. The transparent sealing film was obtained from Thermo Fisher. The microcontroller (ESP32, Espressif Systems) and CMOS camera (OV2640, OmniVision Technologies) were purchased from Digi-Key Electronics. The LED board was custom-made with an array of 12 blue LEDs (732-4966-1-ND) and LED drivers (HV9803BLG-GCT-ND, Digi-Key Electronics). The excitation (FGB25) and emission filters (FGL530) were obtained from Thorlabs Inc.. New England Biolabs Inc. supplied the LAMP reagent kit (E1700S) containing Bst 2.0 DNA polymerase, ddNTPs, SYBR green dye, and isothermal amplification buffer. Finally, the genomic DNA purification kit and LAMP primers were ordered from Promega Corp. and Integrated DNA Technologies, separately.

2.2. Paper microfluidics for LAMP

The paper-based LAMP sensor consists of two layers of papers sealed in a plastic cassette, as illustrated in Fig. 1. To prevent sample evaporation during a LAMP assay, the paper layers were sealed inside the plastic case, as shown in Fig. 1(a). The plastic case was assembled using a perforated acrylic sheet, two layers of papers, and clear sealing tapes. The acrylic sheet was 1.5 mm thick and punched with seven 3-mm-diameter holes that were used as the sample inlet and reaction chambers. The glass microfiber paper (top panel of Fig. 1(b)) with a pore size of 5 μm and thickness of 1.5 mm was used to store the LAMP reagent and house the isothermal amplification reactions. The glass microfiber paper was punched to produce 3-mm-diameter pads, in which lyophilized LAMP reagents and primers were stored. Compared to a cellulose paper substrate, the glass microfiber paper exhibits low background fluorescence, which is desirable for the fluorescence detection of PCR amplicons. The 400-μm-thick polyethersulfone (PES) membrane (bottom panel of Fig. 1 (b)) was chosen to connect the inlet to multiple glass microfiber pads because of the relatively high sample flow rate. Table S1 in the Supplementary Information compares the sample flow rate and background fluorescence signals of three types of paper substrates. The PES microfluidic layer was cut into 1-mm-wide channels using an electronic cutting machine (CM350, Brother). The glass microfiber pads and patterned PES membrane were placed inside the reaction chambers and below the acrylic sheet, respectively. The top and bottom sides of the paper sensor chip were sealed using clear plastic tape. While the sensor chip's main cost is on the LAMP reagents, the chip is considered a consumable that can be disposed of after use.

2.3. IoT-based LAMP detector

During a LAMP reaction, the target sequence can be amplified at a constant temperature using two or three sets of primers. The amplification produced can be measured using the fluorescence signal generated by intercalating dyes, such as SYBR green, whose emission intensity can be correlated to the concentration of the amplicon. To facilitate the real-time measurement of SYBR green emission during a LAMP reaction, we designed a portable LAMP detector, as shown in Fig. 2(a). The compact system offers three main functions, including temperature management, fluorescence detection, and data transmission to a cloud storage. The fluorescence detector, consisting of the blue LED array ($P_{out} = 360$ mW), CMOS camera, and optical filters, was built to measure the emission of SYBR green dye, which is specific to double-stranded DNAs (dsDNAs). As shown in Fig. 2(b), the excitation and emission filters were cut to donut ring and circular disk, respectively, and then joined using an optical adhesive. The filter set was placed in front of the assembly of the camera and the LED array. The fluorescence detector was controlled using the ESP32 microcontroller, which can turn on/off the LEDs, acquire images from the CMOS camera, and transfer the images to the cloud data storage. A Google Apps Script was developed to upload the images to Google Drive *via* a WiFi network. The temperature control unit consists of a thermoelectric cooler (TEC) and a thermocouple (K-type, Omega Engineering). The TEC was powered using a DC power supply, which was switched by the ESP32 microcontroller. During LAMP experiments, the temperature was maintained at 65 °C, and fluorescence images were captured every 1 min and transmitted to the

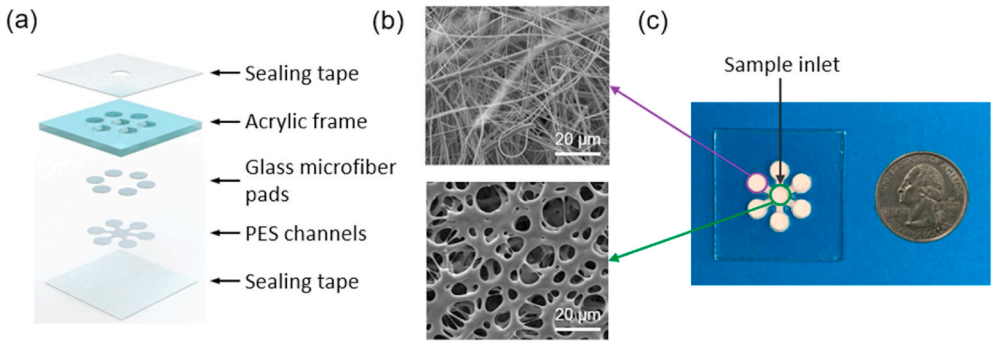

Fig. 1. Design of the paper-based LAMP chip. (a) Schematic of the sensor chip with one inlet and six reaction chambers. (b) Scanning electron microscopy (SEM) images of the glass microfiber (top panel) and PES membrane (bottom panel). (c) Assembled LAMP sensor cassette consisting of six sample chambers and an inlet hole. Each sample chamber contains a paper reaction pad and the inlet. The reaction chambers and inlet are connected by a paper-based liquid flow channel.

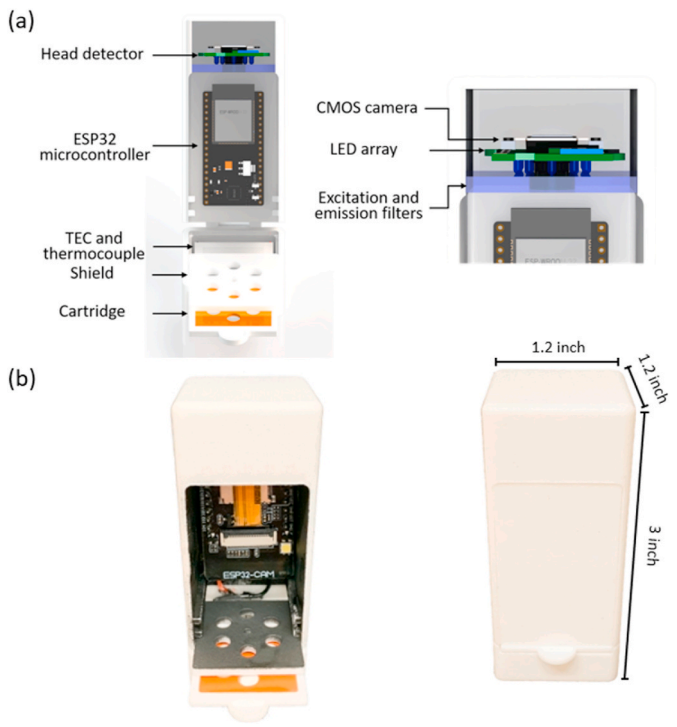

Fig. 2. IoT-based LAMP detector. (a) Schematic design illustrating the housing, temperature management component, microcontroller, and fluorescence detection optics. (b) Photograph of the setup and installed optical and electronic components. The dimension is 1.2"×1.2"×3". The total weight is less than 300 g.

Google Drive folder. The housing for the fluorescence image and temperature was built using a 3D printer to block unwanted ambient light.

2.4. Data collection and processing

A Python script was developed to calculate the SYBR green emission from each reaction pad. The script can extract the green channel of RGB images, filter background noise, identify the reaction pads using the K-means clustering algorithm (Likas et al., 2003). For each image, the average fluorescence intensities within the reaction chambers were calculated and subtracted by the background intensities. The average fluorescence intensity was plotted as a function of time to generate the LAMP amplification curve for each chamber. The amplification curve was analyzed to determine the value of time to threshold (T_t), which is commonly used to quantify the genomic DNA concentration (Nixon et al., 2014). The T_t value is defined as the time when the fluorescence intensity reaches 10% of the maximum fluorescence value. To calculate the T_t value, the LAMP amplification curve was fitted using a four parameters logistic function, $I(t) = \frac{I_{max}-I_0}{1+e^{-(t-t_{1/2})/k}} + I_0$, where $I(t)$ is the fluorescence intensity as a function of time, I_0 represents the initial fluorescence intensity, I_{max} denotes the final fluorescence intensity, $t_{1/2}$ is the time when the half of $I_{max} - I_0$ is reached, and $1/k$ corresponds to the amplification rate. The T_t value was subsequently calculated using $I(T_t) = 0.1 \times (I_{max} - I_0) + I_0$, which corresponds to the 10% increase of fluorescence intensity during an LMAP reaction.

2.5. Preparation of genomic DNAs and LAMP reagent

E. coli (DH5α strain) was cultured at 37 °C in lysogeny broth (LB). *C. jejuni* (IA3902 strain) was cultured on Mueller-Hinton (MH) agar at 42 °C. The bacterial cells were collected by centrifugation for genomic DNA extraction. The genomic DNA was extracted through cell lysis, precipitation, and purification using a genomic DNA purification kit (Promega). The concentrations of purified genomic DNAs were measured using the NanoDrop (Thermo Fisher Scientific). The genomic DNA σs were diluted to the desired concentration for LAMP tests. Three sets of LAMP primers for the *malB* and *tuf* genes of *E. coli* and the *cj0414* gene of *C. jejuni* were previously reported (Hill et al., 2008; Kumar and Mondal, 2015; Yamazaki, 2013). The primer sequences were listed in Table S2 of the Supplementary Information. The primers were dissolved to the desired concentrations and mixed with the LAMP reagent kit. The final concentrations of out forward primer (F3), out reverse primer (B3), forward loop primer (LF), reverse loop primer (LB), forward inner primer (FIP), and reverse inner primer (BIP) were 0.2 μM, 0.2 μM, 0.4 μM, 0.4 μM, 1.6 μM, 1.6 μM, respectively.

3. Results and discussion

3.1. Sample transportation via paper

The paper sensor chip was designed to measure multiple target genes by connecting the sample inlet with multiple reaction chambers using the patterned PES layer. During a test, the sample containing genomic DNAs can be pipetted into the inlet (Fig. 1(a)) and flow to the glass microfiber pads *via* the PES fluidic channels. The glass microfiber pads function as the absorbent layer to enable capillary action to pull the sample into the reaction chambers for LAMP reaction and detection. Fig. 3(a) showcases the sample loading and flow processes using green ink. As shown in Fig. 3(a), the green ink solution, with a volume of 40 μL, started to wick into the reaction chambers after 2 min. It took approximately 4 min for the liquid solution to fill the entire glass microfiber pads. After the primers and LAMP reagents stored inside glass microfiber pads were fully wetted, the ESP32 microcontroller can start LAMP reactions. The rapid sample transportation into different reaction chambers facilitates the simultaneous detection of multiple target genes.

3.2. LAMP analysis on paper

3.2.1. Real-time measurement of isothermal amplification

For LAMP-based assays, the T_t value is commonly used to determine template concentration and enable a quantitative analysis. In order to calculate the T_t value, the amplicons produced by a LAMP reaction need to be measured in real-time to plot the amplification curve. The IoT-based fluorescence detector, as shown in Fig. 2, was developed to facilitate the measurement and analysis of fluorescence emission from SYBR dye, whose emission represents the concentration of the double-stranded DNA (dsDNA) amplicons. As an example, the real-time LAMP detection of the *E. coli malB* gene in the paper substrate was investigated. Before the test, the LAMP reagents, three primer pairs, and *E. coli* genomic DNA at a concentration of 1×10^5 copies/μL were mixed and flowed into the reaction chambers. The paper sensor chip was completely wetted by a sample volume of 50 μL. The sensor chip was heated using the TEC and its temperature was measured using the thermocouple to maintain the chip at the LAMP reaction temperature of 65 °C. During the LAMP assay, the fluorescence images were recorded every 1 min and transferred to the cloud using a WiFi network. Fig. 3(b) shows the sampled fluorescence images acquired at 10 min, 30 min, and 50 min, individually. The increase of the fluorescence emission from the reaction chambers suggests the increase of dsDNA copies. The average fluorescence intensity at each reaction chamber was calculated to generate the amplification curve, as shown in Fig. 3(c). The data points of the amplification curve were fitted with a goodness of fit $R^2 = 0.965$. Following the T_t calculation equation, the T_t and $I(T_t)$ values were 24 min and 38 cts., respectively. As a reference, the same LAMP assay exhibited a T_t of 13 min when the assay was performed in a solution using a benchtop thermocycler. The result shows that the paper-based sensor in conjunction with the IoT-based isothermal PCR reader is feasible for real-time LAMP analysis.

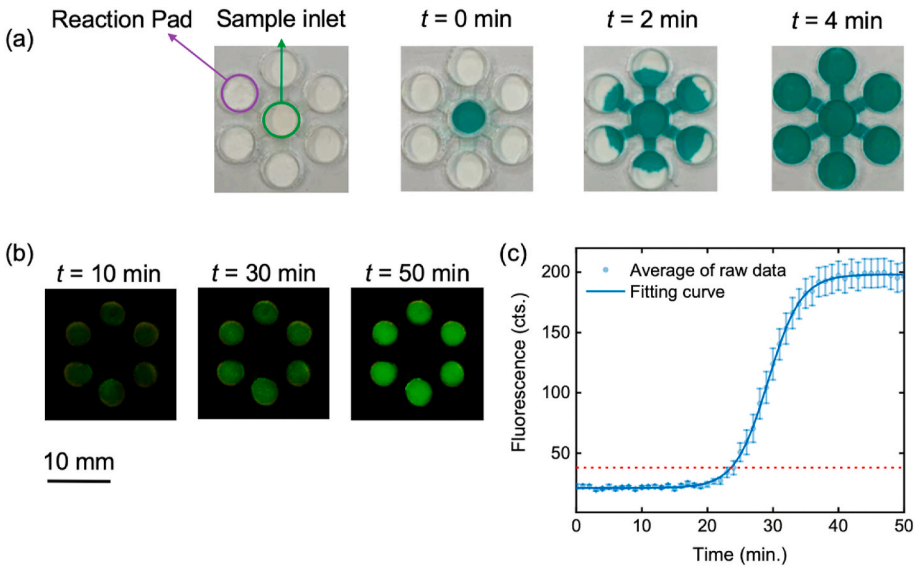

Fig. 3. Paper sensor chip for LAMP detection. (a) Photographs taken when the sample of green ink was filled in the inlet and flowed to the reaction chambers through the PES channels. (b) Fluorescence images recorded during a LAMP test at t = 10 min, 30 min, 50 min, independently. (c) LAMP amplification curve plotted by the fluorescence intensity as a function of reaction time with the deviation of six samples. Measured data points were fitted to determine the fluorescence threshold for finding T_t value, as shown by the red dashed line. (For interpretation of the references to color in this figure legend, the reader is referred to the Web version of this article.)

3.2.2. Quantitative detection of the malB gene in E. coli

Following the demonstration of the real-time detection capability, we proceeded to examine the paper-based LAMP platform for the quantitative detection of a target gene. The genomic DNA sample extracted from the *E. coli* culture was diluted to five different template concentrations ranging from 2×10^3 to 2×10^7 copies/μL. A No Template Control (NTC) sample was included to monitor potential contamination or primer-dimer formation. The mixed solutions of the genomic DNA sample, primer pairs, and LAMP reagents were directly pipetted into the reaction chamber to soak the glass microfiber reaction pads completely. The LAMP titration tests were repeated five times using five different paper sensor chips. For each sensor chip, five chambers were filled with DNA and LAMP reagents and the other one was filled with only LAMP reagents as NTC sample.

Fig. 4(a) shows the fluorescence images of the sensor chip with the reaction pads labeled by circles, which corresponds to different genomic DNA concentrations and the NTC sample. The images were acquired at t = 10, 20, 30, and 40 min after the sensor temperature was stabilized at 65 °C. It is evident that the fluorescence intensities from the reaction pads with genomic DNA samples increased as a function of time. In contrast, there was no change in the fluorescence signal from the NTC sample. Before the amplification reached saturation after 40 min, the chamber with a higher template concentration exhibited a stronger fluorescence signal. Fig. 4(b) compares the amplification curves of the genomic DNA titration, as well as the NTC sample. All samples with DNA templates were successfully amplified and there was no amplification for the NTC sample. The T_t values are 25.5, 24, 21.5, 18.6, and 16.1 min, for template concentrations of 10^3, 10^4, 10^5, 10^6, and 10^7 copies/μL, severally. Fig. 4(c) plots the T_t values as a function of the genomic DNA concentration. The sample pad containing a higher concentration of the template DNA showed a shorter T_t value. The T_t data points were fitted used a linear function with the R^2 coefficient of 0.995. To calculate the limit of detection (LOD), six NTC samples were measured and their T_t values were determined. The average (μ_{NTC}) and standard deviation (σ_{NTC}) of NTCs' T_t values are 53.75 min and 9.23 min, respectively. When the $T_r = \mu_{Tt} - 3\sigma_{Tt}$ = 26.06 min, the LOD corresponds to the

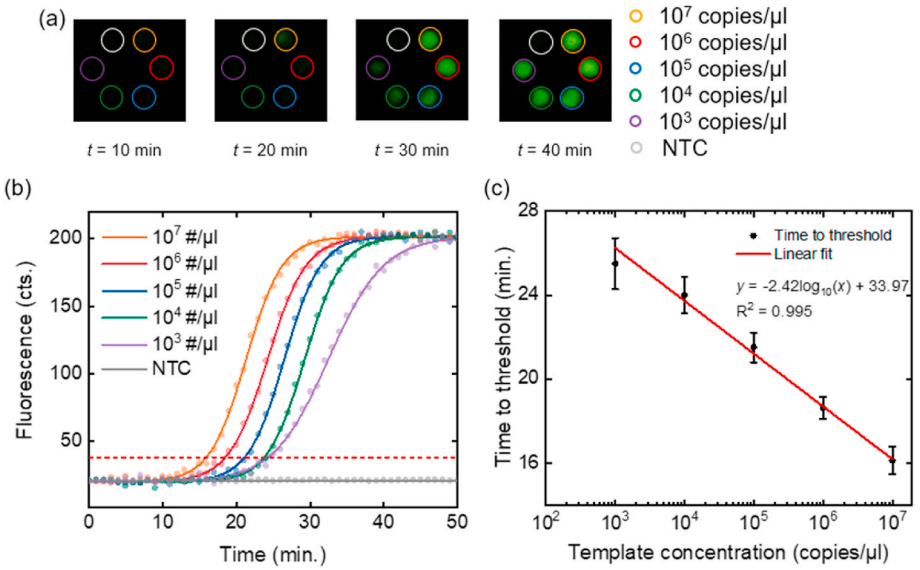

Fig. 4. Quantitative LAMP analysis. (a) Fluorescence images recorded every 1 min during a LAMP amplification. Reaction chambers were filled by samples with different template concentrations. (b) Averaged amplification curves after 5 times experiment for the samples with different template concentrations and the NTC. (c) T_t values extracted from amplification curves with the data set range.

template concentration of 2×10^3 copies/μL based on the linear fit shown in Fig. 4(c).

3.2.3. LAMP amplification using reagents stored in paper

To be able to detect multiple target genes simultaneously, the sensor chip needs to store a specific set of LAMP primers in each reaction chambers. In addition, the storage of assay reagents in the reaction pad will also benefit the applications in resource-limited settings. We studied and optimized the dehydration process to dry LAMP reagents, including the LAMP primer set, DNA polymerase, SYBR green dye, dNTPs, and $MgCl_2$, in the microfiber reaction pad. A stabilizer, trehalose, was added to the LAMP reagents at 5% (v/v ratio) to protect the DNA polymerase. Four different dehydration methods, including lyophilization, evaporation, bake, and vacuum bake processes, were tested. As illustrated in Fig. 5(a), the glass microfiber reaction pads were soaked with the LAMP reagents and subsequently dehydrated using a freezing dryer, desiccator, hotplate (at 50 °C), and vacuum oven (at 50 °C), individually. After the reaction pads were completed dried, they were stored at room temperature (22 °C) for 24 h before testing. The *E. coli* DNA sample with a concentration of 1×10^5 copies/μL was added into the inlet and flowed into the reaction chambers to wet reaction pads and dissolve the dehydrated reagents.

Fig. 5(b) compares the LAMP amplification curves obtained with the stored LAMP reagents for the *malB* gene. The curves are normalized in Fig. 5(c) to calculate the T_t values. It is definitely obvious that the dehydration method plays a key role in the LAMP assay performance, in particular, the T_t value. The end-point fluorescence intensities and T_t values are compared in Fig. 5(d) and **(e)**, respectively. As a reference, the detection of the *malB* gene was also performed using the reagent in wet conditions without any dehydration process. It can be seen from Fig. 5 that the lyophilized sample showed the best performance among these drying methods. The lyophilized sample's T_t value and fluorescence intensity are 32% longer and 22% lower, individually. On the other hand, the evaporation and baking resulted in an increase of the T_t value by 247% and a decrease of the final fluorescence intensity by 52%. These numbers suggest that the lyophilization process can preserve the LAMP regents and keep DNA polymerase activity in paper. The capability of storing LAMP reagents and primers in paper enabled the detection of multiple target genes from one or many pathogens.

3.3. Multiplex LAMP detection on paper

With the LAMP primer sets stored in each reaction pad, it is possible to detect multiple genes. In this study, the paper sensor chip includes six reaction chambers and thus can measure up to six different genes by dehydrating a specific LAMP primer pairs in each chamber. Here, the *malB* and *tuf* genes from *E. coli*, and the *C. jejuni* were chosen. The primer sets for these genes are mixed with LAMP reagents and stored in different reaction pads using the lyophilization process. The sequences for these primers are listed in Table S2 in the Supplementary Information. The genomic DNA samples of *E. coli* and *C. jejuni* were extracted from cell cultures and mixed to the concentrations of 1×10^5 copies/μL and 8×10^4 copies/μL for *E. coli* and *C. jejuni*, respectively. The mixture was pipetted into the inlet (Fig. 1(a)) and flowed to all six reaction pads through the PES channels. Two nearby reaction chambers were used for each gene.

Fig. 6(a) presents the fluorescence images captured during the LAMP assay at $t = 10$, 20, and 40 min, independently. Evidently, the fluorescence intensities from all three reactions increased but at different speeds. The *tuf* gene was first amplified and the *cj0414* gene had the longest T_t value. Fig. 6(b) compares the amplification curves for all three genes. The paper-based LAMP assays for the *malB*, *tuf*, and *cj0414* genes

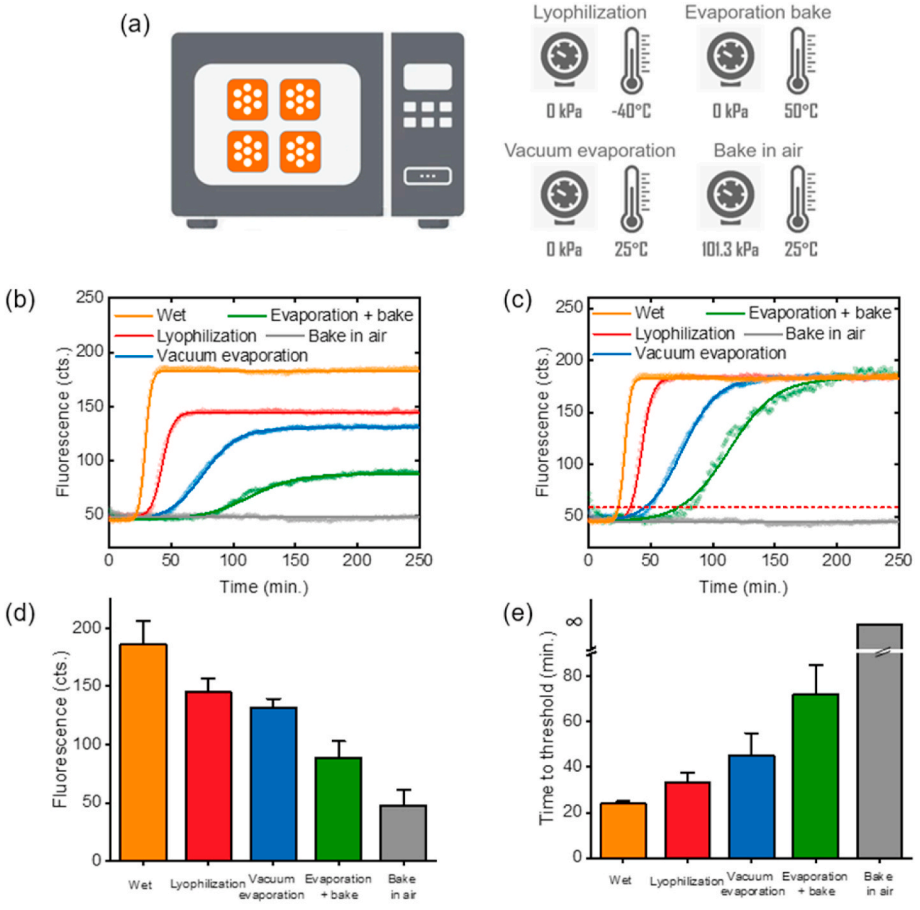

Fig. 5. Dehydration of LAMP regents in paper. (a) Schematics of four dehydration methods. (b) Amplification curves of the *malB* gene using the LAMP reagents stored in the reaction pad by four different dehydration methods. (c) Normalized amplification curves. The end-point fluorescence intensities and T_t values are compared in (d) and (e), severally. The wet sample without dehydration is referred to show the effect of dehydration. Each dehydration method was tested with one paper-based chip with six samples to extract the average and deviation of amplification curves.

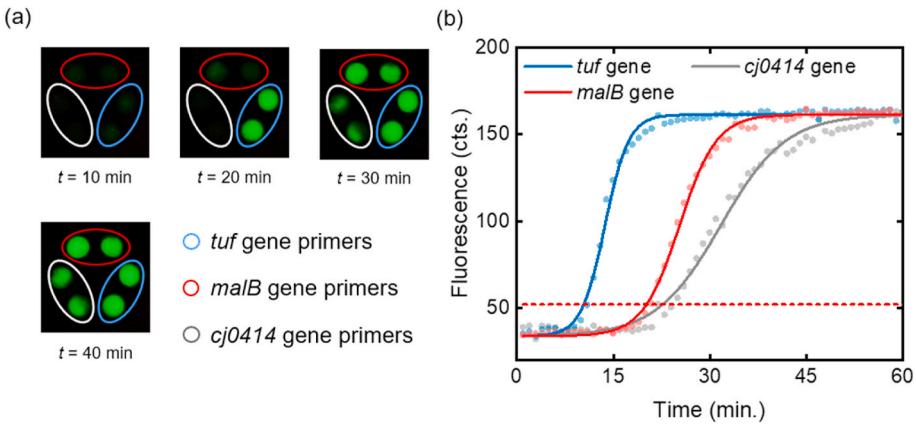

Fig. 6. Simultaneous detection of multiple genes. (a) Fluorescence images captured by the compact device. (b) The amplification curves generated by the data processing program.

exhibit T_t values of 10, 20, and 23 min, respectively. The result shows that the paper sensor chip can be used to develop multiplexed LAMP assay for the detection of multiple target genes from different pathogens.

4. Conclusions

In summary, this work leveraged the advantages of the porous paper substrate to develop the paper-based LAMP sensor chip that is compatible with the compact detector for real-time detections and IoT-based analysis. Two types of paper substrates were used to store LAMP reagents, host isothermal reactions, and transport genomic DNA samples, respectively. The results demonstrated that the paper-based sensor chip can detect multiple target genes from different pathogenic bacteria. The paper-based LAMP sensor exhibited a detection limit as low as 2×10^3 copies/μL and a dynamic range from 10^3 to 10^7 copies/μL. The real-time analysis of fluorescence images, which were recorded *via* the IoT-based fluorescence reader, enabled the quantitative analysis of multiple genes. Such a POC LAMP system can be applied to identify pathogenic organisms for rapid and early-stage diagnosis of infectious diseases. In addition to disease diagnosis, the system also has great potential in forensic and environmental applications.

So far, the paper-based LAMP still has a few limitations. One of them is the lack of DNA purification *in situ*. The LAMP analysis can be significantly simplified by integrating the DNA extraction function into the paper-based sensor chip. Filter papers, such as the fast technology analysis (FTA) paper, have been successfully used to lyse cells or viruses, denature proteins, and extract DNA/RNA molecules from various samples (Tian et al., 2018). The FTA paper can be inserted at the inlet of the paper sensor chip and connected to the LAMP reaction chambers *via* the PES fluidic channels. The nucleic acid extraction function would eliminate extra user operation and achieve a fully automated LAMP assay. The sensor chip can be further improved by patterning the paper substrate using wax printing to reduce the reaction chamber size and increase the number of genes to be tested. Besides the updates on sensor hardware, a browser-based graphical user interface may be developed based on the Google App Script to deliver test results, including the amplification curves and T_t values for each gene, to end-users without the requirement of a specific device.

CRediT author contribution statement

Mingdian Liu: Methodology, Software, Investigation, Writing - original draft, Writing-Original draft preparation. **Yuxin Zhao:** Validation, Resources. **Hosein Monshat:** Software. **Zheyuan Tang:** Methodology. **Zuowei Wu:** Resources, Writing - review & editing. **Qijing Zhang:** Writing - review & editing, Project administration, Funding acquisition. **Meng Lu:** Conceptualization, Methodology, Supervision, Writing - review & editing, Writing, Project administration, Funding acquisition.

Declaration of competing interest

The authors declare that they have no known competing financial interests or personal relationships that could have appeared to influence the work reported in this paper.

Acknowledgments

This research was supported by the National Science Foundation under grant ECCS 16–53673, and the National Institute of Food and Agriculture under Award No. 2018-67021-27968. Any opinions, findings, and conclusions or recommendations expressed in this material are those of the author(s) and do not necessarily reflect the views of the National Science Foundation.

Appendix A. Supplementary data

Supplementary data to this article can be found online at https://doi.org/10.1016/j.bios.2020.112651.

References

Bedin, F., Boulet, L., Voilin, E., Theillet, G., Rubens, A., Rozand, C., 2017. J. Med. Virol. 89, 1520–1527.
Burns, M.A., Johnson, B.N., Brahmasandra, S.N., Handique, K., Webster, J.R., Krishnan, M., Sammarco, T.S., Man, P.M., Jones, D., Heldsinger, D., 1998. Science (80-.) 282, 484–487.
Chan, C.P.Y., Mak, W.C., Cheung, K.Y., Sin, K.K., Yu, C.M., Rainer, T.H., Renneberg, R., 2013. Annu. Rev. Anal. Chem. 6, 191–211.
Cheng, C., Martinez, A.W., Gong, J., Mace, C.R., Phillips, S.T., Carrilho, E., Mirica, K.A., Whitesides, G.M., 2010. Angew. Chem. Int. Ed. 49, 4771–4774.
Choi, J.R., Hu, J., Tang, R., Gong, Y., Feng, S., Ren, H., Wen, T., Li, X., Abas, W.A.B.W., Pingguan-Murphy, B., 2016. Lab Chip 16, 611–621.
Chu, S., Wang, H., Ling, X., Yu, S., Yang, L., Jiang, C., 2020. ACS Appl. Mater. Interfaces 12, 12962–12971.
Cinti, S., Basso, M., Moscone, D., Arduini, F., 2017a. Anal. Chim. Acta 960, 123–130.
Cinti, S., Minotti, C., Moscone, D., Palleschi, G., Arduini, F., 2017b. Biosens. Bioelectron. 93, 46–51.
Cordray, M.S., Richards-Kortum, R.R., 2012. Am. J. Trop. Med. Hyg. 87, 223–230.
Craw, P., Balachandran, W., 2012. Lab Chip 12, 2469–2486.
Ge, X., Asiri, A.M., Du, D., Wen, W., Wang, S., Lin, Y., 2014. TrAC Trends Anal. Chem. (Reference Ed.) 58, 31–39.
Gootenberg, J.S., Abudayyeh, O.O., Kellner, M.J., Joung, J., Collins, J.J., Zhang, F., 2018. Science (80-.) 360, 439–444.
Hill, J., Beriwal, S., Chandra, I., Paul, V.K., Kapil, A., Singh, T., Wadowsky, R.M., Singh, V., Goyal, A., Jahnukainen, T., Johnson, J.R., Tarr, P.I., Vats, A., 2008. J. Clin. Microbiol. 46, 2800–2804.
Hossain, S.M.Z., Luckham, R.E., McFadden, M.J., Brennan, J.D., 2009. Anal. Chem. 81, 9055–9064.
Hu, J., Wang, S., Wang, L., Li, F., Pingguan-Murphy, B., Lu, T.J., Xu, F., 2014. Biosens. Bioelectron. 54, 585–597.

Kaur, N., Toley, B.J., 2018. Analyst 143, 2213–2234.
Kiechle, F.L., Holland, C.A., 2009. Clin. Lab. Med. 29, 555–560.
Kumar, S., Mondal, K.K., 2015. J. Food Sci. Technol. 52, 7417–7424.
Lafleur, L.K., Bishop, J.D., Heiniger, E.K., Gallagher, R.P., Wheeler, M.D., Kauffman, P., Zhang, X., Kline, E.C., Buser, J.R., Kumar, S., 2016. Lab Chip 16, 3777–3787.
Lee, H.H., Dineva, M.A., Chua, Y.L., Ritchie, A., Ushiro-Lumb, I., Wisniewski, C.A., 2010. J. Infect. Dis. 201, S65–S71.
Lee, S.H., Kim, S.-W., Kang, J.Y., Ahn, C.H., 2008. Lab Chip 8, 2121–2127.
Li, B., Zhang, W., Chen, L., Lin, B., 2013. Electrophoresis 34, 2162–2168.
Li, C., Vandenberg, K., Prabhulkar, S., Zhu, X., Schneper, L., Methee, K., Rosser, C.J., Almeide, E., 2011. Biosens. Bioelectron. 26, 4342–4348.
Likas, A., Vlassis, N., Verbeek, J.J., 2003. Pattern Recogn. 36, 451–461.
Magro, L., Escadafal, C., Garneret, P., Jacquelin, B., Kwasiborski, A., Manuguerra, J.-C., Monti, F., Sakuntabhai, A., Vanhomwegen, J., Lafaye, P., 2017. Lab Chip 17, 2347–2371.
Niemz, A., Ferguson, T.M., Boyle, D.S., 2011. Trends Biotechnol. 29, 240–250.
Nixon, G.J., Svenstrup, H.F., Donald, C.E., Carder, C., Stephenson, J.M., Morris-Jones, S., Huggett, J.F., Foy, C.A., 2014. Biomol. Detect. Quantif. 2, 4–10.
Parolo, C., Merkoçi, A., 2013. Chem. Soc. Rev. 42, 450–457.
Petralia, S., Conoci, S., 2017. ACS Sens. 2, 876–891.
Seok, Y., Joung, H.-A., Byun, J.-Y., Jeon, H.-S., Shin, S.J., Kim, S., Shin, Y.-B., Han, H.S., Kim, M.-G., 2017. Theranostics 7, 2220.
Shah, P., Zhu, X., Li, C., 2013. Expert Rev. Mol. Diagn. 13, 83–91.
St John, A., Price, C.P., 2014. Clin. Biochem. Rev. 35, 155.
Syedmoradi, L., Gomez, F.A., 2017. Bioanalysis 9 (11), 841-843.
Tian, T., Bi, Y., Xu, X., Zhu, Z., Yang, C., 2018. Anal. methods 10, 3567–3581.
Wang, H., Da, L., Yang, L., Chu, S., Yang, F., Yu, S., Jiang, C., 2020. J. Hazard Mater. 392.
Wang, H., Yang, L., Chu, S., Liu, B., Zhang, Q., Zou, L., Yu, S., Jiang, C., 2019. Anal. Chem. 91, 9292–9299.
Wang, Y., Zhang, C., Chen, X., Yang, B., Yang, L., Jiang, C., Zhang, Z., 2016. Nanoscale 8, 5977–5984.
Wang, Y., Zhu, Y., Yu, S., Jiang, C., 2017. RSC Adv. 7, 40973–40989.
Yamazaki, W., 2013. Springer, pp. 267–277.
Yan, J., Ge, L., Song, X., Yan, M., Ge, S., Yu, J., 2012. Chem. Eur J. 18, 4938–4945.
Yetisen, A.K., Akram, M.S., Lowe, C.R., 2013. Lab Chip 13, 2210–2251.
Yu, J., Ge, L., Huang, J., Wang, S., Ge, S., 2011. Lab Chip 11, 1286–1291.
Zhang, Y., Zuo, P., Ye, B.-C., 2015. Biosens. Bioelectron. 68, 14–19.
Zhao, C., Thuo, M.M., Liu, X., 2013. Sci. Technol. Adv. Mater. 14, 54402.
Zhou, M., Yang, M., Zhou, F., 2014. Biosens. Bioelectron. 55, 39–43.

Preflight Results

Document Overview

Title: An IoT-enabled paper sensor platform for real-time analysis of isothermal nucleic acid amplification tests
Author: Mingdian Liu
Creator: Elsevier
Producer: Acrobat Distiller 8.1.0 (Windows)

Preflight Information

Profile: Convert to PDF/A-1b
Version: Qoppa jPDFPreflight v2020R2.00
Date: Mar 17, 2021 1:25:57 PM

Legend: (X) - Can NOT be fixed by PDF/A-1b conversion.
(!X) - Could be fixed by PDF/A-1b conversion. User chose to be warned in PDF/A settings.

Page 3 Results

(X) Font widths must be the same in both the font dictionary and the embedded font file.
(X) Font widths must be the same in both the font dictionary and the embedded font file.
(X) Font widths must be the same in both the font dictionary and the embedded font file.